

## A genetic algorithm with neural network fitness function evaluation for IMRT beam angle optimization

Joana Dias · Humberto Rocha ·  
Brígida Ferreira · Maria do Carmo Lopes

© Springer-Verlag Berlin Heidelberg 2013

**Abstract** Intensity Modulated Radiotherapy Treatment (IMRT) is a technique used in the treatment of cancer, where the radiation beams are modulated by a multileaf collimator allowing the irradiation of the patient using non-uniform radiation fields from selected angles. Beam angle optimization consists in trying to find the best set of angles that should be used in IMRT planning. The choice of this set of angles is patient and pathology dependent and, in clinical practice, most of the times it is made using a trial and error procedure or simply using equidistantly distributed angles. In this paper we propose a genetic algorithm that aims at calculating good sets of angles in an automated way, given a predetermined number of angles. We consider the discretization of all possible angles in the interval  $[0^\circ, 360^\circ]$ , and each individual is represented by a chromosome with 360 binary genes. As the calculation of a given individual's fitness is very expensive in terms of computational time, the genetic algorithm uses a neural network as a surrogate model to calculate the fitness of most of the individuals in the population. To explicitly consider the estimation error that can result from the use of this surrogate model, the fitness of each individual is represented by an interval of values and not by a single crisp value. The genetic algorithm is capable of finding improved solutions, when compared to the usual equidistant solution applied in clinical practice. The genetic algorithm will be described and computational results will be shown.

---

J. Dias  
Faculdade de Economia, Universidade de Coimbra, Coimbra, Portugal

J. Dias (✉) · H. Rocha  
Inesc-Coimbra, Coimbra, Portugal  
e-mail: joana@fe.uc.pt

B. Ferreira · M. do Carmo Lopes  
Serviço de Física Médica, IPOC-FG, EPE, Coimbra and Departamento de Física,  
Universidade de Aveiro, I3N, Aveiro, Portugal

20 **Keywords** Genetic algorithms · Radiotherapy · IMRT · Surrogate model ·  
 21 Neural networks

Author Proof

## 22 **1 Introduction**

23 The goal of radiation therapy is to deliver a dose of radiation to the cancerous region  
 24 to sterilize the tumor minimizing the damages to the surrounding healthy organs and  
 25 tissues. Radiation therapy is delivered with the patient immobilized on a couch that can  
 26 rotate around a vertical axis. For most types of cancer, radiation therapy is administered  
 27 5 days each week for 5–8 weeks (Lim 2008). Using small radiation doses daily instead  
 28 of few larger doses helps protect healthy tissues in the tumor region. Typically, high  
 29 energy photon beam radiation is generated by a linear accelerator mounted on a gantry  
 30 that can rotate along a central axis (Fig. 1) parallel to the couch. The rotation of the  
 31 couch combined with the rotation of the gantry allows radiation from almost any angle  
 32 around the tumor. The aim is to be able to plan a treatment that is in accordance with  
 33 the medical prescription in terms of radiation dose distribution. Usually, the medical  
 34 prescription will define prescribed doses to the target volumes (the regions that have to  
 35 be irradiated), and mean or maximum tolerance doses to the organs at risk (the regions  
 36 that should be spared). Despite the fact that almost all angles can be used in radiation  
 37 delivery, the use of coplanar angles (without couch rotation) is the most usual option.  
 38 This is a way to simplify an already complex problem, and the angles considered lie  
 39 in the plane of the rotation of the gantry around the patient. Regardless the evidence  
 40 presented in the literature that appropriate radiation beam incidence directions can  
 41 lead to a plan's quality improvement (Das and Marks 1997; Liu et al. 2006), in clinical  
 42 practice, most of the time, the number of beam angles is assumed to be defined *a priori*  
 43 by the treatment planner and the beam directions are still manually selected by the  
 44 treatment planner who relies mostly on his experience.

45 An important type of radiation therapy is intensity modulated radiation therapy  
 46 (IMRT), where the radiation beams are modulated by a multileaf collimator. Multileaf  
 47 collimators enable the transformation of the beam into a grid of smaller beamlets of  
 48 independent intensities, as illustrated in Figs. 2 and 3. Here, we will consider IMRT  
 49 optimization problems using coplanar angles and we will assume that the number of  
 50 beam angles is defined *a priori* by the treatment planner.

51 The decision-making process regarding IMRT treatment planning can be concep-  
 52 tually understood as having three main steps.

- 53 1. Beam Angle Optimization (BAO): deciding what is the best number of beam angles  
 54 and their directions. This means deciding how many times does the gantry stop,  
 55 and where should it stop.
- 56 2. Fluence Map Optimization (FMO): deciding which are the best beamlet intensities  
 57 for each gantry position. This means calculating the optimal radiation intensity  
 58 profile that will be delivered to the patient every time the gantry stops, so that the  
 59 medical prescription is satisfied.
- 60 3. Leaf Sequencing Problem: determining how the leaves of the multileaf collimator  
 61 should move, so that the optimal beamlet intensities calculated in the previous step  
 62 are, in fact, delivered.

**Fig. 1** Linear accelerator



**Fig. 2** Illustration of an MLC (with nine pairs of leaves)

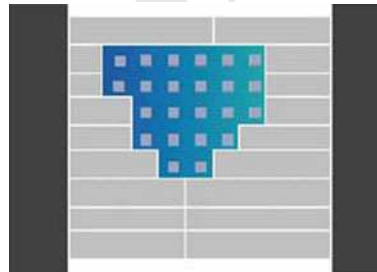
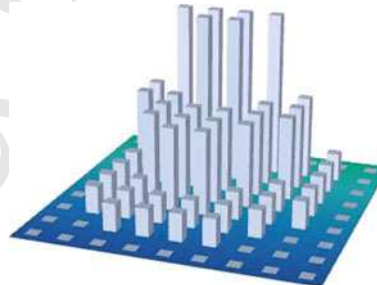


**Fig. 3** Illustration of a beamlet intensity map ( $9 \times 9$ )



63 There are approaches that try to consider a beamlet-based approach, without the need  
64 to look at this problem using this three step framework, but those approaches lead to  
65 the development of large-scale optimization problems.

66 Most of the efforts in the IMRT optimization community have been devoted at  
67 optimizing beamlet intensities (Craft 2007), and comparatively fewer research effort  
68 has been directed to the optimization of beam angles (Ehrgott et al. 2008).

69 The BAO problem has been tackled using several different methodologies: scoring  
70 methods, where scores are assigned to beam angles based on geometric and dosimetric  
71 information (D'Souza et al. 2004); methods based on the concept of beam's eye view  
72 (Goitein et al. 1983; Lu et al. 1997; Pugachev and Xing 2001a,b), where the area of  
73 the tumor and the area of the surrounding organs as seen by the beam are considered  
74 in the selection of the better candidates; response surface approach (Aleman et al.

75 2006); derivative-free approaches (Rocha et al. 2012); mixed integer programming  
76 approaches (Lee et al. 2006); among others (see, for instance, Das and Marks 1997;  
77 Ehrgott and Johnston 2003; Craft 2007; Lim and Cao 2012).

78 Many authors have also applied metaheuristics to this problem like simulated  
79 annealing (Bortfeld and Schlegel 1993; Lu et al. 1997; Djajaputra et al. 2003) or  
80 particle swarm optimization (Li et al. 2005). Evolutionary algorithms have also been  
81 used. Wu et al. (2000), consider conformal radiotherapy treatment planning, and use  
82 a genetic algorithm to determine beam intensities. Li et al. (2004), describe a genetic  
83 algorithm where each chromosome has as many genes as angles that are encoded  
84 using integers. Schreibmann et al. (2004), describe a hybrid multiobjective evolution-  
85 ary algorithm that produces a set of efficient solutions for the multiobjective problem  
86 considered. Li and Yao (2006), use a genetic algorithm hybridized with an ant colony  
87 approach applied to BAO. Li et al. (2006), describe a genetic algorithm with a small  
88 population (the number of individuals is double the number of beams considered), that  
89 makes use of plan templates provided by experts. Bevilacqua et al. (2007), develop a  
90 genetic algorithm that can be applied to conformal, aperture-based and IMRT treat-  
91 ments, with the genetic representation changed accordingly. Lei and Li (2008), Li and  
92 Lei (2010), describe a genetic algorithm applied to the beam selection problem where  
93 the representation of each individual is based on the DNA structure. A small population  
94 of 24 individuals is used in chest and oropharyngeal tumor examples. Nazareth et al.  
95 (2009), describe the use of a genetic algorithm that is run on a distributed computing  
96 platform such that each generation takes about 30 min to be completed. Holdsworth  
97 et al. (2010), consider a two level multiobjective optimization evolutionary algorithm  
98 where the lower level performs a deterministic beamlet intensity optimization using  
99 a weighted quadratic objective function, and the top level uses a randomly generated  
100 population of individuals to represent the objective function weights that determine the  
101 relative weighting between organs to spare and targets. Fiege et al. (2011), describe the  
102 application of a parallel multiobjective genetic algorithm (*Ferret*) to BAO and FMO.  
103 They demonstrate the feasibility of the proposed approach on two phantoms (artificial  
104 models used to simulate the effect of radiation). Other genetic algorithm applications  
105 in radiotherapy treatment planning that do not deal explicitly with BAO can also be  
106 found (Lahanas et al. 2003; Haas and Reeves 2005).

107 The BAO problem is the first problem that should be solved in treatment planning,  
108 but in reality its optimal solution will be dependent on the optimal solutions of the two  
109 other sequential problems, especially on the optimal solution of the FMO. We need  
110 to know what are the optimal beamlet intensities associated with each set of angles  
111 to be able to compare different solutions (see, for instance, Das and Marks 1997;  
112 Haas et al. 1998; Schreibmann et al. 2004; Aleman et al. 2006; Craft 2007). When the  
113 BAO problem is not based on the optimal FMO solutions, the resulting beam angle  
114 set has no guarantee of optimality and has questionable reliability since it has been  
115 extensively reported that optimal beam angles for IMRT are often non-intuitive (Stein  
116 et al. 1997). Obtaining the optimal solution for a beam angle set is time costly and  
117 even if only one beam angle is changed in that set, a complete dose computation is  
118 required in order to compute and obtain the corresponding optimal FMO solution.  
119 This can cause a serious problem if we intend to use algorithms that require several  
120 objective function evaluations, as is the case with evolutionary algorithms, and we

121 have limited computational resources as is the case in many health institutions. One  
122 way of overcoming this problem is to use a surrogate model to calculate an estima-  
123 tion of the true objective function value. This idea has been used by several authors  
124 in different environments (see, for instance, El-Beltagy and Keane 1999; Emmerich  
125 et al. 2002; Jin and Sendhoff 2004; Jin and Branke 2005), but has never been applied  
126 to BAO.

127 The main contribution of this paper is to introduce the use of surrogate models within  
128 an evolutionary algorithm framework applied to BAO. We present a genetic algorithm  
129 that considers a discretization of the interval of all possible angles and that uses a neural  
130 network as surrogate model to calculate the fitness function of most individuals in the  
131 population. The algorithm uses the standard genetic operators (selection, crossover,  
132 mutation) as well as migration and a special local search operator that is nothing more  
133 than a genetic algorithm considering a very small elite population.

134 The paper is organized as follows: in the next section we describe the BAO problem  
135 formulation and the associated FMO problem formulation. Section 3 describes the  
136 surrogate model used. Section 4 describes the genetic algorithm. Clinical examples  
137 of head-and-neck cases used in the computational tests and some computational and  
138 clinical results are presented in Sect. 5. Section 6 presents the conclusions and some  
139 guidelines for future work.

## 140 2 Beam angle optimization problem

141 In beam angle optimization we aim at finding the best set of beams to be used in a given  
142 treatment. This means calculating the optimal number of beams,  $k$ , and figuring out  
143 what are the best  $k$  beam angles. This is a very important step in IMRT optimization  
144 since it directly influences both the quality of the treatment delivered and the overall  
145 treatment time. The treatment time increases with the increase in the number of beams.  
146 From the institution's point of view, fewer beams means that more patients can be  
147 treated. From the patient point of view, the faster the treatment the better because it  
148 is more likely that the patient does not change his position significantly during the  
149 treatment, which contributes to more accurate treatment results.

150 In this paper we consider that  $k$  is determined *a priori*. For each set of  $k$  beams, we  
151 will need to determine a way of assessing the *goodness* of this set. This assessment  
152 can only be done after considering how the radiation dose will be deposited into the  
153 patient cells, so the FMO problem needs to be first solved so that we can consider  
154 the optimized beamlet intensities for each beam. To solve the FMO problem, we need  
155 a way to calculate accurately the radiation dose distribution deposited in the patient,  
156 measured in Gray (Gy). Each structure's volume is discretized in voxels (small volume  
157 elements) and the dose is computed for each voxel using the superposition principle,  
158 i.e., considering the contribution of each beamlet. Typically, a dose matrix  $D$  is such  
159 that each row of  $D$  corresponds to a voxel and each column to each possible beamlet.  
160 Thus, the number of rows of matrix  $D$  equals the number of voxels ( $V$ ) and the number  
161 of columns equals the number of beamlets ( $N$ ) from all beam directions considered.  
162 The element in row  $i$  and column  $j$  of matrix  $D$  corresponds to the dose contribution  
163 to voxel  $i$  from beamlet  $j$  with unit intensity. Therefore we can say that the total dose

164 received by the voxel  $i$  is given by  $\sum_{j=1}^N D_{ij}w_j$ , with  $w_j$  representing the intensity  
 165 (or fluence) of beamlet  $j$ . Usually, the total number of voxels considered reaches the  
 166 tens of thousands, thus the row dimension of the dose matrix is of that magnitude.  
 167 The size of  $D$  originates large-scale problems being one of the main reasons for the  
 168 difficulty of solving the FMO problem. From a mathematical point of view, we are  
 169 thus in the presence of two related problems. If we define  $\Theta$  as the set of all possible  
 170 angles, then a basic formulation for the BAO problem can be defined as follows:

$$171 \quad \min f(\theta_1, \theta_2, \dots, \theta_k) \quad (1)$$

$$172 \quad \text{subject to } \theta_1, \dots, \theta_k \in \Theta \quad (2)$$

173 If we consider a discretization of  $\Theta$  then we are in the presence of a combinatorial  
 174 optimization problem.

175 There is no consensual way of calculating optimal beamlet intensities. Many mathe-  
 176 matical optimization models and algorithms have been proposed for the FMO problem,  
 177 including linear models (Romeijn et al. 2003), mixed integer linear models (Lee et al.  
 178 2003), nonlinear models (Cheong et al. 2005), and multiobjective models (Craft et al.  
 179 2006). We have chosen to use a convex penalty function voxel-based nonlinear model  
 180 (Aleman et al. 2008). According to this model, each voxel is penalized considering  
 181 the square difference of the amount of dose received by the voxel and the amount of  
 182 dose desired/allowed for the voxel. This formulation yields a quadratic programming  
 183 problem with only linear nonnegativity constraints on the fluence values (Romeijn et  
 184 al. 2003):

$$185 \quad \text{Min}_w \sum_{i=1}^V \left[ \lambda_i \left( T_i - \sum_{j=1}^N D_{ij}w_j \right)_+^2 + \bar{\lambda}_i \left( \sum_{j=1}^N D_{ij}w_j - T_i \right)_+^2 \right] \quad (3)$$

$$186 \quad \text{s.t. } w_j \geq 0, \quad j = 1, \dots, N \quad (4)$$

187 where  $T_i$  is the desired dose for voxel  $i$ ,  $\lambda_i$  and  $\bar{\lambda}_i$  are the penalty weights of underdose  
 188 and overdose of voxel  $i$ , respectively, and  $(\cdot)_+ = \max\{0, \cdot\}$ .

189 Although this formulation allows unique  $\lambda_i$  and  $\bar{\lambda}_i$  weights associated with each  
 190 voxel, similarly to the implementation in Aleman et al. (2008), weights are assigned  
 191 by structure only so that every voxel in a given structure has the weight assigned to that  
 192 structure divided by the number of voxels of the structure. This nonlinear formulation  
 193 implies that a very small amount of underdose or overdose may be accepted in clinical  
 194 decision making, but larger deviations from the desired/allowed doses are decreasingly  
 195 tolerated. It is beyond the scope of this study to discuss if this formulation of the FMO  
 196 problem is preferable to others or not.

### 197 3 Surrogate model

198 For each set of  $k$  beam angles we will need to solve a FMO problem. The computational  
 199 time spent solving one single instance of the FMO is dependent on the patient and

200 on  $k$ , but it is always computationally expensive. Table 2 shows the computational  
201 times in seconds of solving one instance of the FMO quadratic programming problem.  
202 Depending on the patient and number of beams considered, it can take from 40 s to more  
203 than 5 min to solve a single FMO optimization problem. This makes it difficult to use  
204 algorithms that require many objective function evaluations, like genetic algorithms.

205 To try and overcome this difficulty, it is possible to use a surrogate model, that will  
206 be able to estimate the true objective function value in a tiny fraction of time than it  
207 takes to calculate its true value.

208 In this work, we have decided to use a neural network (NN) to map sets of angles  
209 into objective function values. The use of NNs in radiotherapy problems is not new.  
210 Willoughby et al. (1996), describe the use of a NN to model the clinical judgment made  
211 by physicians when assessing treatment plans. Wells and Niederer (1998), develop an  
212 expert system based on NNs to plan standardized 3D conformal therapy treatments.  
213 Knowles et al. (1998), describe the use of NNs that will return the required treatment  
214 plan parameters after being trained (using evolutionary algorithms) with completed  
215 treatment plans. Rowbottom et al. (1999), consider prostate cancer patients treated with  
216 conformal therapy, and develop a NN that receives as inputs the patients' geometry  
217 information and has as outputs the angles' configuration. Gulliford et al. (2004), try  
218 to predict biological outcomes in prostate cancer patients after being submitted to  
219 radiotherapy treatments. Mathieu et al. (2005) and Vasseur et al. (2008), describe  
220 the use of NNs for accurate and fast dose calculation. Llacer et al. (2009), use NNs  
221 as part of an automatic non-coplanar beam orientation selection. The NNs work as  
222 classifiers, creating beam clusters based on the beam's coverage of the tumor to be  
223 treated plus some safety margins, and are also used for the geometric definition of the  
224 patient. Kalantzis et al. (2011), investigate the use of NNs in reconstructing dose maps  
225 for IMRT, achieving good results. For an introduction to NNs and a survey of NNs  
226 applied to radiotherapy problems see, for instance, Goodband and Haas (2008).

227 The main idea used in our work is as follows: we want to train a patient specific  
228 NN, that will receive sets of angles as inputs and that, for one particular patient, will  
229 return as output the value of the FMO objective function (3).

230 First of all, it will be necessary to generate a set of samples. Sets of  $k$  randomly  
231 generated angles are considered, and for each of these sets the true value of the objective  
232 function,  $f$ , is computed by calculating the optimal solution of the FMO problem.  
233 These samples are then used to train a neural network. The trained neural network is  
234 then ready to calculate  $f'$  expecting this value to be as close to  $f$  as possible (Fig.  
235 4). This neural network should be capable of mapping a highly non-linear surface,  
236 with many local minima (Fig. 5). To facilitate the training of neural networks, and  
237 to improve their performance, both inputs and outputs are often normalized to lie in  
238 a fixed range (see, for instance, Shanker et al. 1996; Witten and Frank 2005; Han  
239 and Kamber 2006, pp. 70–72). We applied a normalization procedure as follows:  
240 considering the input angles, we decided to subtract  $180^\circ$  to each angle value and then  
241 divide by  $180^\circ$ , so that all angle values are within the interval  $[-1, 1]$ . Regarding the  
242 output values, their statistical mean and standard deviation were calculated, the mean  
243 was subtracted from each value and the result was divided by the standard deviation.  
244 This results in a set of values with mean approximately equal to zero and standard  
245 deviation approximately equal to one.

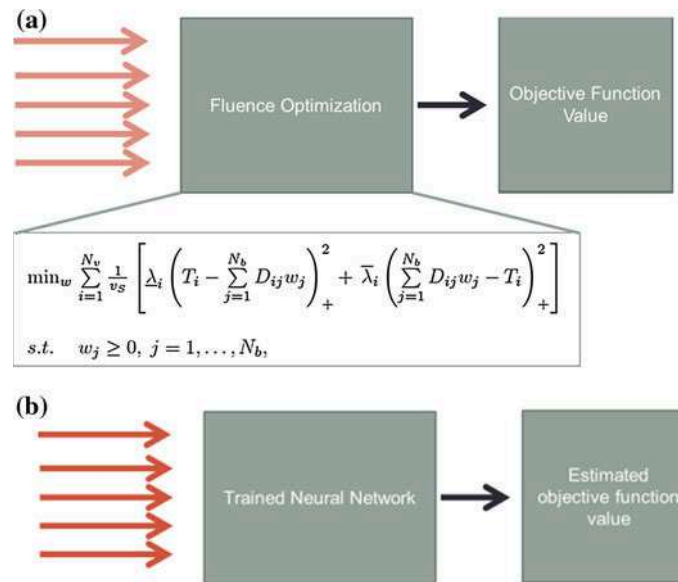


**Fig. 4** Considering sets of 5 angles, the neural network will have five inputs (one input for each of the angles) and will have as output the estimated objective function value. **a** while training; **b** after training

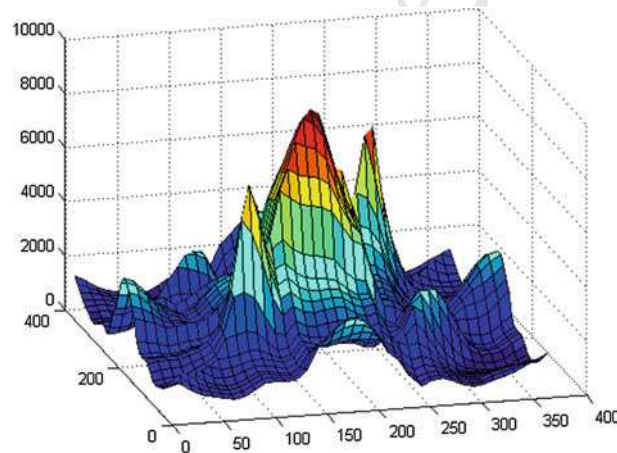


**Fig. 5** Example of the objective function surface (defined by Eq. (3)) when we are considering sets of two angles only

246 It is not easy to decide on the best neural network architecture to use, and it is  
 247 expected that this best architecture will be dependent on the particular situation at hand  
 248 (the patient, the medical prescription, the number of angles, the number of samples  
 249 available to train the NN).

250 For this reason, several neural network configurations are tested before choosing  
 251 the best one. This is done as follows:



**Fig. 6** An example of a neural network with three inputs (*three angles*), two hidden layers with four neurons each and one output (objective function value)

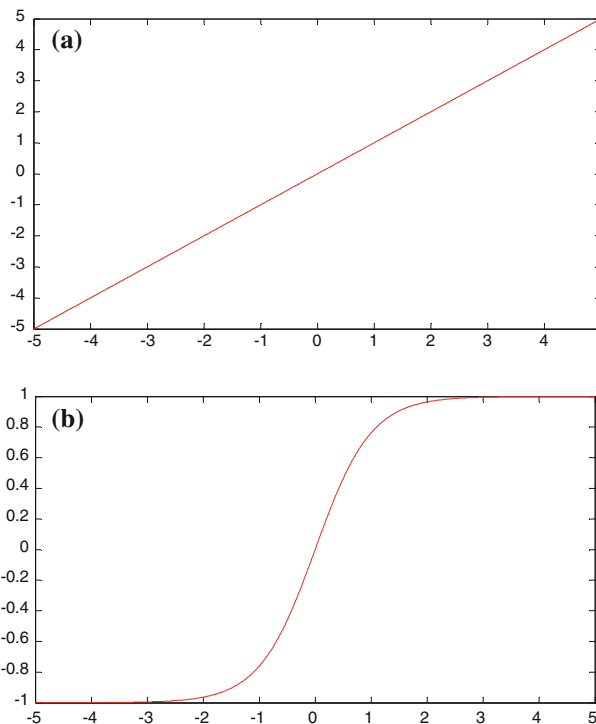
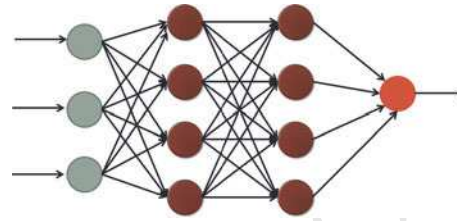


**Fig. 7** **a** Linear transfer function; **b** Hyperbolic tangent sigmoid transfer function

- 252 1. Divide the set of available samples into three sets: training set (60%), cross-validation set (20%) and test set (20%).
- 253
- 254 2. For each NN configuration, train the network using the samples in the training set, and calculate the estimation error using the cross-validation set. The estimation error is calculated by averaging the squared differences between each estimated value calculated by the NN and the corresponding target value from the cross-validation set.
- 255
- 256
- 257
- 258
- 259 3. Choose the NN configuration with the least estimation error.
- 260 4. Train 20 NNs with the same configuration chosen at step 3, randomly initialized.
- 261 5. Calculate the outputs for each of the 20 trained NNs using the test set, and consider the estimated values equal to the average value of all NN estimations. Calculate the expected estimation error using the test set.
- 262
- 263

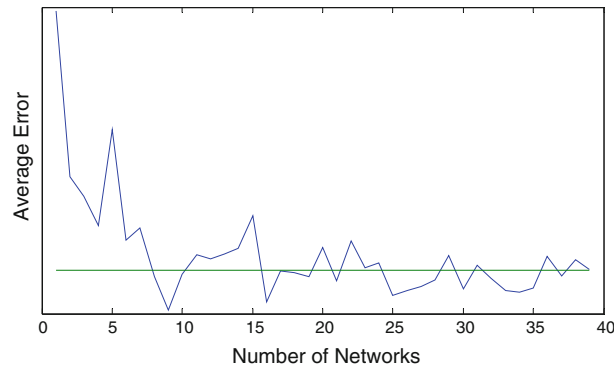


**Fig. 8** Estimation error diminishes with the increase in the number of NNs

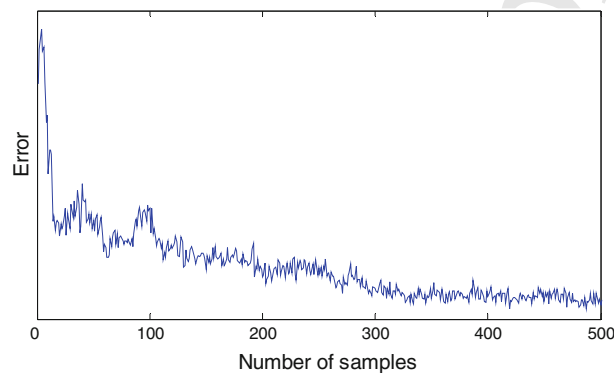


**Fig. 9** Learning curve

264 The configurations tested in step 2 consider 1 to 5 hidden layers, and 1 to 40 neurons  
 265 in each hidden layer (all hidden layers with the same number of neurons—Fig. 6). All  
 266 hidden layers will have hyperbolic tangent sigmoid transfer functions, and the output  
 267 layer will have a linear transfer function (Fig. 7).

268 The reasoning of using not a single NN but a set of 20 different NNs has to do with  
 269 the fact that this can contribute to a decrease in the estimation error (Fig. 8).

270 As would also be expected, the error decreases with the increase in the number of  
 271 available training samples (Fig. 9).

#### 272 **4 Genetic algorithm**

273 The genetic algorithm developed considers the BAO problem as a combinatorial opti-  
 274 mization problem, where the interval of all possible angles is discretized into 360  
 275 possible degrees. This makes it trivial to think of each individual (solution) as being  
 276 represented by a chromosome constituted by 360 binary genes: if a gene is equal  
 277 to one then the corresponding angle is used in the treatment, otherwise it is not. As  
 278 the number of angles to be used is fixed *a priori* and is equal to  $k$ , this means that

279 each individual will have exactly  $k$  genes equal to one. The initial population will be  
280 randomly generated. As several sets of angles were already generated so that the NN  
281 could be trained, we take advantage of these individuals and use them as the initial  
282 population.

283 Two angles that are  $4^\circ$  or less apart from each other are considered similar from a  
284 clinical point of view. If a given individual has two angles that are less than  $4^\circ$  apart,  
285 then one of these angles is randomly chosen to be deleted (the corresponding gene  
286 is set to zero), and another randomly chosen gene is changed to 1. The procedure  
287 is repeated until there are no angles that are  $4^\circ$  or less apart. All individuals, in all  
288 generations, are submitted to such a procedure, so that we can guarantee that every  
289 individual will have angles that are at least  $4^\circ$  apart.

#### 290 4.1 Fitness evaluation

291 For each individual in the population we can either calculate its fitness value by solving  
292 the FMO problem or by using the surrogate model. In the latter case, there will probably  
293 be an estimation error associated with the fitness value. This is why each individual  
294 will not have a single and crisp fitness value but its fitness will be represented by  
295 an interval. Each time the neural network is trained, we calculate the mean and the  
296 standard deviation of the estimation error using the test set. If we represent by  $\mu$   
297 the mean error and by  $\sigma$  the standard deviation, then if there were  $n$  samples in  
298 the test set and, for a given individual, the estimated fitness is given by  $f'$ , then the  
299 individual's fitness interval will be equal to  $[f' + \mu - 1.96 \frac{\sigma}{\sqrt{n}}, f' + \mu + 1.96 \frac{\sigma}{\sqrt{n}}]$ . If  
300 the real fitness value is calculated using (3)–(4), then the upper and lower limit of this  
301 interval will be equal to the true fitness value.

302 It is not trivial to choose between using the original but computationally expensive  
303 objective function value or the surrogate model fitness calculation. It will always be  
304 necessary to calculate the true objective function value for some individuals, otherwise  
305 the function to be optimized will be the one represented by the surrogate model and not  
306 the true objective function. There are authors that consider the calculation of the true  
307 fitness for at least 50 % of all individuals, to guarantee that the evolutionary algorithm  
308 will try to optimize the true objective function (Hüsken et al. 2005). We can think about  
309 individual or generation control procedures (Jin et al. 2002). In the first approach, a  
310 certain number of individuals (*controlled individuals*) are evaluated using the true  
311 objective function in each generation. In the latter, in every  $g$  generations (*controlled*  
312 *generations*), all individuals are evaluated using the original fitness function. In this  
313 paper we have chosen the first approach, mainly due to computational limitations  
314 (the latter is better used when it is possible to use parallelization).

315 In each generation, two individuals are chosen and are passed directly to the next  
316 generation (elitist approach): the one that has the minimum fitness interval lower  
317 bound and the one that has the minimum fitness interval upper bound. Their true  
318 fitness function is calculated (if not known already). The choice of, in each generation,  
319 calculating the true objective value for two individuals, has to do with the fact that  
320 we need to assure the genetic algorithm is trying to reach an optimal solution for the  
321 “true” objective function, and is not optimizing the objective function defined by the  
322 surrogate model.

323 It was tried to maintain a lookup table, that would keep a record of every individual  
 324 with a known true objective fitness function. Then, whenever a new individual was  
 325 generated, the first thing to do would be to check if there is a match in the lookup  
 326 table. Nevertheless, a match occurred in less than 0.5 % of the times, so this option  
 327 was abandoned.

#### 328 4.2 Selection operator

329 The selection operator is responsible for the selection of individuals that will generate  
 330 the offsprings that will constitute the new generation. We have chosen to use the  
 331 tournament selection operator. This means that two individuals are randomly chosen  
 332 from the current population, and their fitness values are compared. The best individual  
 333 is chosen with a given probability. The procedure is repeated so that a second individual  
 334 is chosen. These two individuals are then used to generate two new individuals.

335 As we are considering fitness intervals and not crisp fitness values, if the  
 336 intervals do not overlap, then the comparison between individuals is trivial. If  
 337 we are in the presence of two individuals such that their fitness intervals are,  
 338 respectively,  $\left[ f'_1 + \mu - 1.96 \frac{\sigma}{\sqrt{n}}, f'_1 + \mu + 1.96 \frac{\sigma}{\sqrt{n}} \right]$  and  $\left[ f'_2 + \mu - 1.96 \frac{\sigma}{\sqrt{n}}, f'_2 + \mu \right.$   
 339  $\left. + 1.96 \frac{\sigma}{\sqrt{n}} \right]$  such that  $f'_1 < f'_2$ , then if  $\left( f'_1 + \mu + 1.96 \frac{\sigma}{\sqrt{n}} \right) < \left( f'_2 + \mu - 1.96 \frac{\sigma}{\sqrt{n}} \right)$   
 340 we can conclude that individual 1 has a better fitness than individual 2. If this does not  
 341 happen, meaning that  $\left( f'_1 + \mu + 1.96 \frac{\sigma}{\sqrt{n}} \right) \geq \left( f'_2 + \mu - 1.96 \frac{\sigma}{\sqrt{n}} \right)$ , then the fitness  
 342 intervals overlap and we have to see if it is possible to conclude whether the fitness  
 343 values are comparable or not (Knezevic 2008). If  $(f'_2 - f'_1) > 1.96 \frac{\sigma}{\sqrt{n}} \sqrt{2}$  we consider  
 344 that individual 1 has a better fitness than individual 2, otherwise we consider that we  
 345 cannot reach a conclusion and we choose randomly one of them to participate in the  
 346 crossover operator.

#### 347 4.3 Crossover operator

348 The crossover operator used is as follows: each pair of parents will generate two twins.  
 349 Each twin will have all angles belonging to each of the parents (Fig. 10). As we must  
 350 have  $k$  and only  $k$  genes equal to one, these twins will correspond to non-admissible  
 351 solutions (unless both parents are identical). So, a random procedure is applied, where  
 352 genes that are equal to one are randomly selected and are changed to zero until  $k$   
 353 angles are reached.

354 Other crossover operators were tried (like one-point and two-point crossover), but  
 355 better results were obtained with this procedure.

#### 356 4.4 Mutation operator

357 Each offspring will, with a given probability, suffer a mutation. This means that one  
 358 randomly chosen gene that is equal to one will be changed to zero, and one randomly  
 359 chosen gene equal to zero will be changed to one.

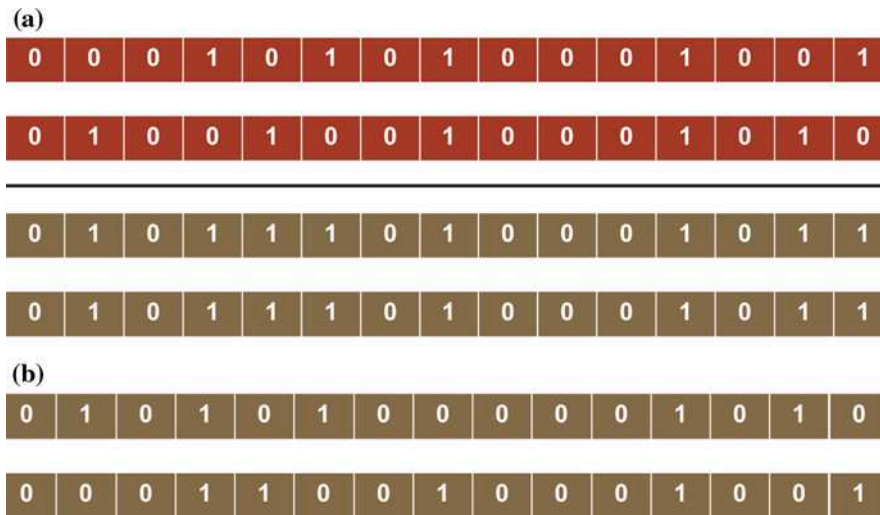


**Fig. 10** Crossover operator **a** the two parents above will generate two twins. **b** these twins will be randomly changed so that only  $k$  genes keep their values equal to 1

#### 360 4.5 Migration

361 Whenever some number of generations is evolved without an improvement in the  
 362 objective function value of the BAO problem, a certain percentage of the population  
 363 is substituted by randomly generated individuals. This procedure can be interpreted  
 364 as a migration using a population with a high mutation rate, and contributes to the  
 365 increase of the population diversity.

#### 366 4.6 Local search

367 After running the described genetic algorithm, a local search procedure is executed.  
 368 This local search procedure is, in fact, another genetic algorithm composed by exactly  
 369 the same procedures of the genetic algorithm described, but with two main differences:  
 370 the population is constituted by a very small number of individuals, and it is initialized  
 371 by considering mutations of the best individual found so far; the fitness of all the  
 372 individuals in this elite population is calculated by solving the FMO problem. Due to  
 373 computational time limitations, the population will only evolve during a small number  
 374 of generations.

#### 375 4.7 Retraining the NN

376 In every generation of the genetic algorithm, the true objective function is calculated  
 377 for the best individuals in the population. This means that these individuals can be  
 378 considered as new samples. From time to time, the NN is retrained using this new  
 379 and enlarged sample set. As the number of training samples increases, the standard  
 380 deviation and the average error are expect to decrease, so that as the genetic algorithm  
 381 evolves better estimations are produced by the surrogate model.

## 382 4.8 The whole picture

383 The complete algorithm is now described:

- 384 1. Generate a set of samples, by randomly generating  $k$  angles and calculating the  
385 corresponding FMO objective function value (3).  
386 2. Find the best NN architecture.  
387 3. Train a set of NNs.  
388 4. Execute the genetic algorithm  
389 a. Initialize the population  
390 b. While the termination condition is not met (maximum time or maximum num-  
391 ber of iterations has not been reached)  
392 i. The true fitness value is calculated for two “best” individuals, that are  
393 immediately passed on to the next generation  
394 ii. Selection  
395 iii. Crossover  
396 iv. Mutation  
397 v. If the objective function does not improve during  $n$  consecutive genera-  
398 tions then migration  
399 vi. If  $m$  new samples have been created, retrain the NNs  
400 5. Execute the local search

401 **5 Computational and clinical results**

402 The described algorithm was tested considering ten clinical examples of already treated  
403 patient cases of head-and-neck tumors at the Portuguese Institute of Oncology of  
404 Coimbra (IPOC). A typical head-and-neck treatment plan consists of radiation deliv-  
405 ered from 5 to 9 equally spaced coplanar orientations around the patient. We consid-  
406 ered treatments with 5 coplanar beams because the importance of beam angle selection  
407 increases when a lower number of beam angles is considered. Furthermore, 5 angles  
408 is the usual starting point for the trial and error procedure conducted by planners.  
409 An increase in the number of angles is only considered if they are unable to reach a  
410 clinically acceptable solution.

411 In order to facilitate convenient access, visualization and analysis of patient treat-  
412 ment planning data, as well as dosimetric data input for treatment plan optimiza-  
413 tion research, the computational tools developed within MATLAB and CERR—  
414 computational environment for radiotherapy research (Deasy et al. 2003) are used  
415 widely for IMRT treatment planning research. The ORART—operations research  
416 applications in radiation therapy (Deasy et al. 2006) collaborative working group  
417 developed a series of software routines that provide the necessary dosimetry data to  
418 perform optimization in IMRT. CERR was elected as the main software platform to  
419 embody our optimization research.

420 Our tests were performed on a Intel Core i7 CPU 2.8 GHz computer with 4GB RAM  
421 and Windows 7. We used CERR 3.2.2 version and MATLAB 7.4.0 (R2007a). The dose  
422 was computed using CERR’s pencil beam algorithm (QIB). For each of the ten head-  
423 and-neck cases, the voxel size considered was  $0.3\text{ cm} \times 0.3\text{ cm} \times 0.3\text{ cm}$ . Table 1

**Table 1** Prescribed doses for all the structures considered for IMRT optimization

Structure	Spinal cord	Brainstem	Left parotid	Right parotid	PTV1	PTV2	Body
Mean dose	–	–	26 Gy	26 Gy	–	–	–
Maximum dose	45 Gy	54 Gy	–	–	–	–	80 Gy
Prescribed dose	–	–	–	–	70 Gy	59.4 Gy	–
# voxels case 1	1,382	1,715	1,576	1,390	4,001	31,119	1,790,592
# voxels case 2	3,567	2,072	1,536	1,807	1,485	43,649	1,413,138
# voxels case 3	3,265	2,087	2,538	2,367	16,860	69,748	1,608,589
# voxels case 4	1,424	1,569	676	684	4,856	28,721	6,64,886
# voxels case 5	1,115	983	1,372	1,265	31,924	2,292	2,073,296
# voxels case 6	1,101	1,518	1,176	1,140	30,047	6,613	1,560,070
# voxels case 7	985	851	668	631	19,835	3,973	1,110,882
# voxels case 8	1,160	1,223	1,405	1,323	29,786	4,450	1,710,982
# voxels case 9	829	1,135	782	1,096	11,348	1,153	1,016,083
# voxels case 10	533	2,907	1,056	662	25,461	11,066	1,553,317

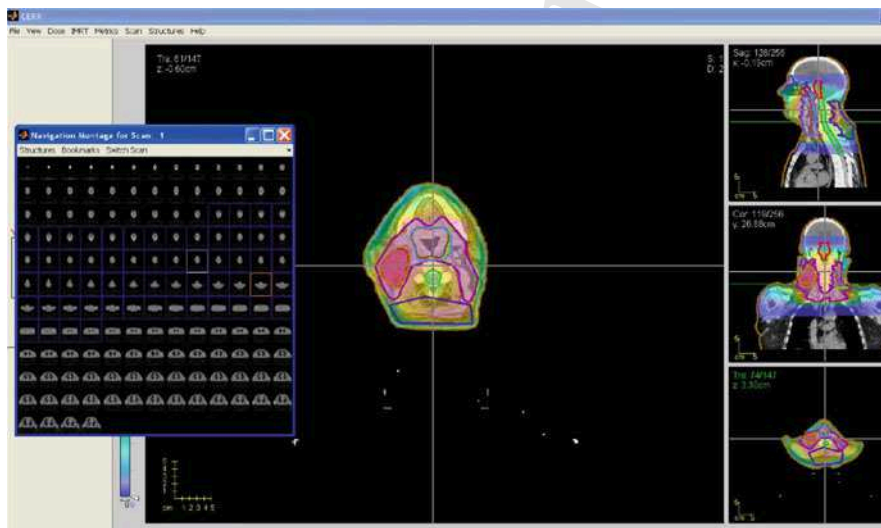
424 presents the number of voxels for each patient and for each structure considered.  
 425 An automated procedure for dose computation for each given beam angle set was  
 426 developed, instead of the traditional dose computation available from CERR's menu  
 427 bar. This automation of the dose computation was essential for integration in our BAO  
 428 algorithm. To address the convex nonlinear formulation of the FMO problem we used a  
 429 trust-region-reflective algorithm (fmincon) of MATLAB 7.4.0 (R2007a) Optimization  
 430 Toolbox. For this set of patients, each instance of the FMO problem can take from  
 431 56 to 350 s to be calculated, depending on the patient and on the set of beam angles  
 432 considered (Table 2).

### 433 5.1 Clinical examples

434 Ten clinical examples of already treated patient cases of head-and-neck tumors at the  
 435 Portuguese Institute of Oncology of Coimbra are used to test the genetic algorithm  
 436 described. The selected clinical examples were signalized at IPOC as complex cases  
 437 where proper target coverage and organ sparing, in particular parotid sparing, proved  
 438 to be difficult to obtain. The patients' CT sets and delineated structures were exported  
 439 via Dicom RT to CERR (see Fig. 11). Since the head-and-neck region is a complex  
 440 area where, e.g., the parotid glands (the two largest salivary glands) are usually in  
 441 close proximity to or even overlapping with the target volume, careful selection of the  
 442 radiation directions can be essential to obtain a satisfying treatment plan. The spinal  
 443 cord and the brainstem are some of the most critical organs at risk (OARs) in the head-  
 444 and-neck tumor cases. These are serial organs, i.e., organs such that if only one subunit  
 445 is damaged, the whole organ functionality is compromised. Therefore, if the tolerance  
 446 dose is exceeded, it may result in functional damage to the whole organ. Thus, it  
 447 is extremely important not to exceed the tolerance dose prescribed for these types of  
 448 organs. Other than the spinal cord and the brainstem, the parotid glands are also impor-

**Table 2** Computational times (in seconds) needed to solve one instance of the FMO quadratic programming problem (considering a sample of 100 instances for each patient)

Patient	5 angles			7 angles			9 angles		
	Min.	Average	Max.	Min.	Average	Max.	Min.	Average	Max.
1	43.20	94.30	102.20	126.51	130.89	137.33	98.48	185.71	226.22
2	56.44	66.17	75.96	81.01	97.61	113.85	136.79	106.98	218.36
3	50.85	117.02	126.70	157.94	169.38	174.12	133.54	235.30	255.91
4	45.68	110.45	122.63	71.00	89.98	101.33	107.55	124.70	142.12
5	89.17	96.64	113.85	122.06	139.38	153.36	170.47	191.95	236.05
6	71.07	82.73	96.16	99.38	121.32	206.72	131.46	157.21	250.99
7	59.20	77.34	91.97	97.35	123.39	152.48	140.24	186.24	227.21
8	78.26	95.33	105.46	124.21	138.98	158.59	157.84	191.27	323.66
9	73.39	91.98	194.84	102.75	128.98	164.13	148.03	185.64	350.94
10	83.60	93.62	103.00	119.23	131.40	147.64	162.98	185.62	228.50

**Fig. 11** CERR environment

449 tant OARs. The parotid glands are the largest of the three salivary glands. A common  
 450 complication due to the irradiation of parotid glands is xerostomia (the medical term  
 451 for dry mouth due to lack of saliva). This decreases the quality of life of patients  
 452 undergoing radiation therapy of head-and-neck, causing difficulties to swallow.

453 The parotids are parallel organs, i.e., if a small volume of the organ is damaged,  
 454 the rest of the organ functionality may not be affected. Their tolerance dose depends  
 455 strongly on the fraction of the volume irradiated. Hence, if only a small fraction of  
 456 the organ is irradiated the tolerance dose is much higher than if a larger fraction is  
 457 irradiated. Thus, for these parallel structures, the organ mean dose is generally used  
 458 instead of the maximum dose as an objective for planning. In general, the head-and-



459 neck region is a complex area to treat with radiotherapy due to the large number  
460 of sensitive organs in this region (e.g., eyes, mandible, larynx, oral cavity, etc.). In  
461 this study, the OARs used for treatment optimization were defined by the medical  
462 physicists as being the spinal cord, the brainstem and the parotid glands. The tumor to  
463 be treated plus some safety margins is called planning target volume (PTV). For the  
464 head-and-neck cases in study it was separated in two parts with different prescribed  
465 doses: PTV1 and PTV2. The prescription dose for the target volumes and tolerance  
466 doses for the organs at risk considered in the optimization are presented in Table 1. The  
467 parotid glands are in close proximity to or even overlapping with the PTV which helps  
468 explaining the difficulty of sparing them. Adequate beam directions are an integral  
469 and important part of IMRT optimization, and can be determinant for achieving the  
470 sparing of parotid glands.

## 471 5.2 Computational results for NN

472 Neural networks were implemented by using the Matlab Neural Network Toolbox.  
473 The surrogate model was tested considering the ten different patients. To assess the  
474 behavior of the model in different settings, we considered five, seven and nine angles.  
475 It is not trivial to determine how should the performance of a surrogate model be  
476 measured, especially when this surrogate model is being used to guide an evolutionary  
477 algorithm (see, for instance, [Hüsken et al. 2005](#)). In this paper we will analyze the  
478 results obtained by considering the relative estimation error, especially looking at its  
479 average value and standard deviation. The results shown in Table 3 consider a training  
480 set of 100 samples. As can be observed, the error standard deviation decreases with  
481 the increase in the number of angles. This means that it will be possible to use fewer  
482 samples when dealing with more angles, without deteriorating in a significant way the  
483 quality of the estimation, as can be seen by looking at Table 4 that considers a training  
484 set of 50 samples.

485 If we try to fit a probability distribution to the estimation errors obtained, most of  
486 the times the normal and the logistic distributions are the most adequate considering  
487 the Anderson-Darling statistic.<sup>1</sup>

## 488 5.3 Computational results for GA

489 In the computational tests for GA we will consider IMRT treatments with five angles.  
490 The genetic algorithm was implemented considering an initial population of 100  
491 individuals (the individuals used to train the initial set of neural networks). The selection  
492 operator will choose the best individual with 80 % probability. We chose to use a  
493 high mutation rate of 50 %. Whenever 25 generations evolve without an improvement  
494 in the objective function value, 25 % of the population is replaced by randomly generated  
495 individuals. The local search procedure considers an initial population of only 10  
496 individuals, created by mutating the best individual found so far, and this population  
497 is evolved during at most 10 generations.

<sup>1</sup> These tests were performed using the fit distribution option of software @Risk.

**Table 3** Computational results for NN (N-Number of neurons in each level; L-number of hidden layers; SD-relative error standard deviation; A-average relative error), 100 samples

	Patient 5 angles				7 angles				9 angles			
	Best NN configuration		Relative error		Best NN configuration		Relative error		Best NN configuration		Relative error	
	N	L	SD (%)	A (%)	N	L	SD (%)	A (%)	N	L	SD (%)	A (%)
1	25	2	14	-2	8	5	9	-1	17	1	7	0
2	33	2	17	2	18	4	12	-1	33	2	8	0
3	20	3	9	0	37	2	6	-1	40	2	6	0
4	21	2	11	0	36	1	6	1	25	1	5	0
5	19	3	10	0	38	1	6	-1	37	2	4	0
6	29	2	15	0	22	2	9	2	30	4	6	0
7	40	2	25	0	16	4	20	9	36	2	13	-1
8	33	2	14	0	39	3	14	-1	35	3	10	0
9	23	2	15	0	28	3	12	0	35	2	8	-1
10	30	2	12	3	26	2	8	1	22	5	6	0

**Table 4** Computational results for NN (N-Number of neurons in each level; L-number of hidden layers; SD-relative error standard deviation; A-average relative error), 50 samples

	Patient 5 angles				7 angles				9 angles			
	Best NN configuration		Relative error		Best NN configuration		Relative error		Best NN configuration		Relative error	
	N	L	SD (%)	A (%)	N	L	SD (%)	A (%)	N	L	SD (%)	A (%)
1	27	2	15	-3	12	4	9	-1	3	4	7	1
2	40	2	20	3	12	3	13	0	10	2	8	1
3	22	5	9	-2	25	1	7	-2	28	2	6	-1
4	10	5	9	1	38	2	7	-1	9	2	5	0
5	16	4	12	0	36	2	6	-2	32	3	5	0
6	31	1	18	-1	5	4	10	0	17	5	6	-1
7	33	2	33	5	1	4	22	14	11	5	13	-3
8	33	1	19	6	33	3	15	-1	30	2	11	0
9	19	4	18	0	40	3	12	1	17	2	9	0
10	29	2	14	4	24	1	8	-2	3	4	7	-1

498 If we want to be able to apply these procedures in a clinical setting, then we have to  
 499 consider some time constraints. It is important that planning the treatment of a given  
 500 patient does not take more than one night. This means that we should consider as a  
 501 time limit more or less 12 h. That is why we have chosen to terminate the genetic  
 502 algorithm when 400 generations are reached or if 10 h have elapsed, whatever occurs  
 503 sooner (notice that the time starts counting with the generation of the sampling sets  
 504 used to train the NN). Then we allow the local search procedure to take at most 2 h.

**Table 5** Computational results for GA

Patient	Average <i>BAO-GA</i> solution	Standard deviation	<i>Equi</i> solution (%)
1	326.98	1.53	4.3
2	66.78	0.01	6.4
3	174.52	0.81	9.0
4	138.28	1.61	8.7
5	244.49	1.23	9.0
6	152.41	0.96	9.8
7	30.86	0.44	10.5
8	134.16	0.20	10.6
9	95.82	0.51	10.7
10	152.84	0.95	6.2

**Table 6** Generating random solutions: computational results

Patient	Best random solution	Standard deviation	<i>Equi</i> solution (%)
1	336.57	5.81	1.5
2	67.70	3.25	5.1
3	182.66	3.28	4.8
4	141.78	2.73	6.4
5	261.83	1.66	2.5
6	162.95	1.37	3.5
7	34.70	1.26	0.0
8	151.10	1.34	0.0
9	103.49	1.00	3.5
10	162.21	4.22	0.5

505 The results of BAO optimization concerning the improvement of the objective  
 506 function value for the ten cases of head-and-neck tumors using our BAO algorithm,  
 507 denoted *BAO-GA* are presented in Table 5. Due to the random nature of the genetic  
 508 algorithm, it is not sufficient to present results considering a single execution of the  
 509 algorithm. We chose to execute the algorithm five times for each patient, and we  
 510 present average and standard deviation results. The fourth column presents the average  
 511 decrease in the objective function value when compared with the traditional 5-beam  
 512 equispaced coplanar treatment plans, denoted *equi*.

513 Using the surrogate model implies the random generation of a set of solutions. It  
 514 could be interesting to compare the results obtained by using the genetic algorithm  
 515 with the results obtained using a simple random generation procedure. To be able to  
 516 draw conclusions, it would not be advisable to compare the results of the GA with  
 517 a single set of random solutions. As calculating the objective function value of each  
 518 solution is very time consuming, we decided to randomly generate and evaluate 300  
 519 solutions. This is our base set. Then, using this set, we consider a random withdrawal of  
 520 100 solutions and calculate the best solution among the 100 solutions. This process is  
 521 then repeated 100 times (so that in each time we get a possibly different sample of 100  
 522 solutions randomly taken from the base set). Table 6 presents the best solution found,  
 523 the standard deviation calculated, and the improvement regarding the *equi* solution.

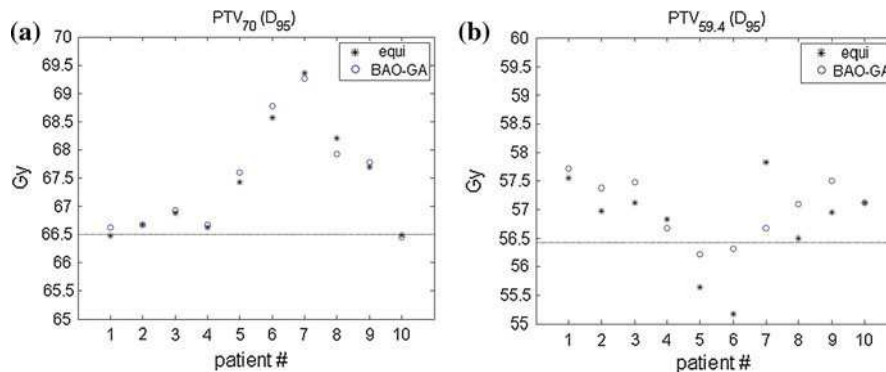


**Fig. 12** Comparison of target irradiation metric obtained by *BAO-GA* and *equi* treatment plans

524 As can be seen, the genetic algorithm presents better results, and also a more reliable  
 525 behavior, since the standard deviations are considerable when applying only a random  
 526 procedure.

527 Since a small standard deviation was obtained for the results of the different runs  
 528 of the *BAO-GA* algorithm, for the remainder of this section we will use the treatment  
 529 plans corresponding to the best *BAO-GA* solution.

530 Despite the improvement in FMO value, the quality of the results can be perceived  
 531 considering a variety of metrics. A metric usually used for plan evaluation is the vol-  
 532 ume of PTV that receives 95 % of the prescribed dose. Typically, 95 % of the PTV  
 533 volume is required. This metric is displayed for the ten cases in Fig. 12. The hori-  
 534 zontal lines represent 95 % of the prescribed dose. Satisfactory treatment plans should  
 535 obtain results above these lines. By simple inspection we can verify the advantage of  
 536 *BAO-GA* treatment plans that have an improved tumor irradiation metric for most cases  
 537 compared to *equi* treatment plans.

538 In order to verify organ sparing, mean and/or maximum doses of OARs are usually  
 539 displayed. For each OAR, the corresponding metric is displayed for the ten cases  
 540 in Fig. 13. The horizontal lines represent the tolerance mean or maximum dose for  
 541 the corresponding structures. Satisfactory treatment plans should obtain results under  
 542 these lines. For spinal cord and brainstem, treatment plans fulfill the maximum dose  
 543 tolerance in all tested cases. However, as expected, the mean dose limit for parotids  
 544 was only achieved few times mostly by *BAO-GA* treatment plans. Moreover, observing  
 545 Fig. 13, it is perceivable that *BAO-GA* treatment plans outperform *equi* treatment plans  
 546 in terms of mean dose obtained. In fact, in average, *BAO-GA* treatment plans reduced  
 547 the mean dose of the parotid glands by 0.96 Gy compared to the *equi* treatment  
 548 plans.

549 Typically, results are judged by their cumulative dose-volume histogram (DVH).  
 550 The DVH displays the fraction of a structure's volume that receives at least a given  
 551 dose. DVH results for the sixth patient illustrate the numbers presented in Fig. 14.  
 552 Since parotids are the most difficult organs to spare, as shown in Fig. 13, for clarity,  
 553 the DVHs only include the targets and the parotids and were split in left and right  
 554 parotid. The asterisks indicate 95 % of PTV volumes versus 95 % of the prescribed

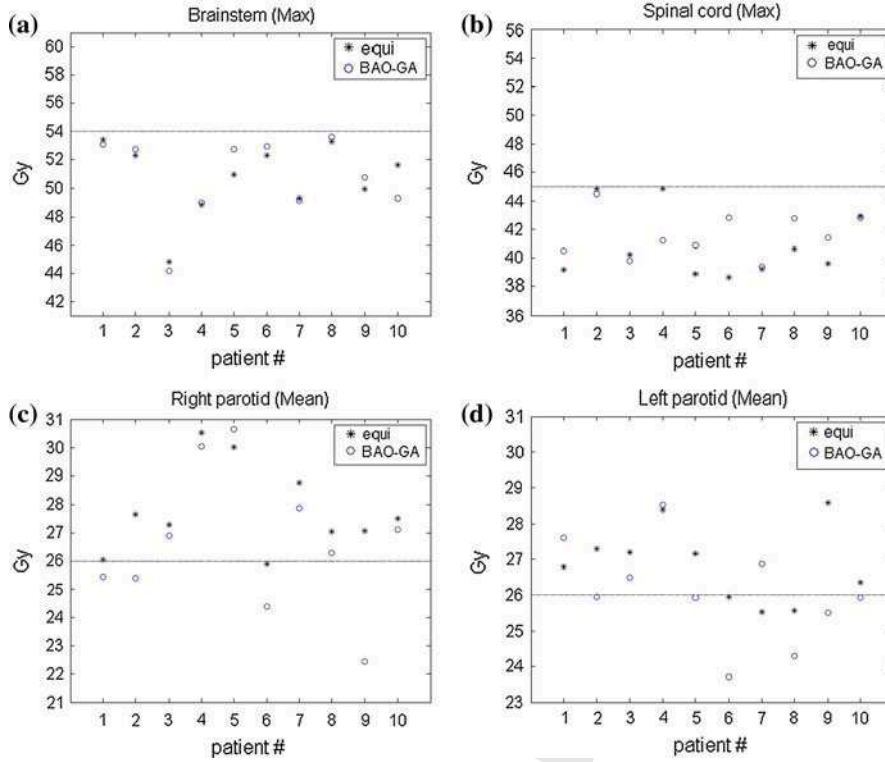


**Fig. 13** Comparison of organ sparing metrics obtained by *BAO-GA* and *equi* treatment plans

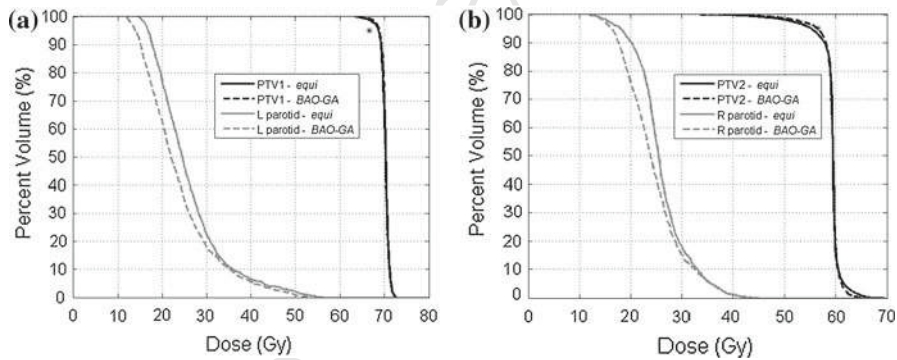


**Fig. 14** Cumulative dose volume histogram comparing the results obtained by *BAO-GA* and *equi* treatment plans for the sixth patient

555 doses. The results displayed in Fig. 14 confirm the benefits of using the optimized  
 556 beam directions, in particular using the directions obtained and used in the *BAO-GA*  
 557 treatment plan.

558 **6 Conclusions and future research**

Author Proof

559 Beam angle optimization in radiotherapy treatment planning, especially in IMRT, can  
560 lead to significant improvements in the quality of treatments delivered to patients. It  
561 can lead to better preservation of the organs at risk, without jeopardizing the treatment  
562 efficacy, leading to an increase in the quality of life of patients. The need for beam  
563 angle optimization increases with the decrease in the number of angles to be used  
564 in a given treatment. Although better results can be expected with an increase in the  
565 number of directions used, using fewer angles is beneficial not only for the patient but  
566 also from the health institution's point of view: fewer angles means faster treatments,  
567 so more patients can be treated; faster treatments means better treatment precision  
568 because the probability of maintaining the patient immobilized in the desired position  
569 with no significant intrafraction setup errors (errors caused by organ motion or patient  
570 position change during treatment) is increased.

571 In this paper we introduce the use of patient dependent surrogate models embedded  
572 into an evolutionary algorithm optimization framework for BAO. The BAO problem  
573 is usually characterized by the existence of many local minima, and a highly nonlinear  
574 optimization surface. Genetic algorithms or evolutionary algorithms in general, are  
575 known to be able to tackle this kind of problems, due to their diversification capabilities  
576 and ability to escape from local minima. Nevertheless, due to the computational time  
577 needed to assess each given individual (solution), that can take from 1 min to more  
578 than 5 min, the use of genetic algorithms may not be compatible with clinical practice,  
579 especially with limited availability of computational resources. In clinical practice we  
580 should take no more than 12 h to generate an improved treatment. To try and overpass  
581 this difficulty, we propose the use of a surrogate model (a trained neural network) that  
582 will be used to calculate the fitness of most individuals in the population.

583 The computational results obtained show that the use of surrogate models combined  
584 with genetic algorithms can be an interesting path of research to follow.

585 Regarding future work, we will consider not only the improvement of the genetic  
586 algorithm, but also try to improve the surrogate model. In the latter case, instead of  
587 considering as inputs the angles, we can consider using scores associated with these  
588 angles (see, for instance, [Pugachev and Xing 2002](#)). The neural network will then  
589 receive information that is expected to be more related with the objective function  
590 value than only the angles. Another possibility is to consider a neural network that,  
591 instead of calculating an estimate of the objective function value, will be able to  
592 compare two individuals stating if one individual is better or worse than the other. As  
593 a matter of fact, in the genetic algorithm evolution, the selection procedure drives the  
594 evolution process, and more than knowing precisely the objective function values we  
595 need a way of comparing individuals in a fast and reliable way (it is more important to  
596 ensure the correct selection than to reproduce exactly the true fitness values—[Hüsken  
597 et al. 2005](#)). Another change would be to consider diminishing the number of times  
598 the real fitness function is calculated as the genetic algorithm evolves, as we will be  
599 dealing with a surrogate model that is improved whenever the neural networks are  
600 retrained.

601 In this paper we consider a discretization of the interval  $[0^\circ, 360^\circ]$  in 360 values. We  
602 now feel that this may be too ambitious. New experiments will be made considering

603 at first a more coarse discretization, and only in later stages considering a larger set of  
604 discretized values.

605 Looking at the FMO problem, and thinking of an evolutionary algorithm, it is  
606 almost inevitable to think of multiobjective approaches to deal with this problem that  
607 is multiobjective by nature: we want to give the prescribed radiation to the target  
608 volumes, and as little radiation as possible to the organs at risk, which in most cases  
609 are contradictory objectives.

610 **Acknowledgments** This work was supported by FEDER funds through the COMPETE program,  
611 by QREN under Mais Centro (CENTRO-07-0224-FEDER-002003), and Portuguese funds through  
612 FCT—Fundação para a Ciência e a Tecnologia, under project PTDC/EIA-CCO/121450/2010 and by FCT  
613 under project grant PEst-C/EEI/UI0308/2011. The work of H. Rocha was supported by the European social  
614 fund and Portuguese funds.

## 615 References

- 616 Aleman D, Romeijn H, Dempsey J (2006) A response surface-based approach to beam orientation opti-  
617 mization in IMRT treatment planning. IIE Annual conference exposition, Orlando, FL, pp 6–11
- 618 Aleman DM, Kumar A, Ahuja RK, Romeijn HE, Dempsey JF (2008) Neighborhood search approaches  
619 to beam orientation optimization in intensity modulated radiation therapy treatment planning. *J Glob*  
620 *Optim* 42(4):587–607
- 621 Bevilacqua V, Mastronardi G, Piscopo G (2007) Evolutionary approach to inverse planning in coplanar  
622 radiotherapy. *Image Vis Comput* 25(2):196–203
- 623 Bortfeld T, Schlegel W (1993) Optimization of beam orientations in radiation therapy: some theoretical  
624 considerations. *Phys Med Biol* 38(2):291–304
- 625 Cheong K, Suh T, Romeijn H, Li J, Dempsey J (2005) Fast nonlinear optimization with simple bounds for  
626 IMRT planning. *Med Phys* 32:1975–1975
- 627 Craft D (2007) Local beam angle optimization with linear programming and gradient search. *Phys Med*  
628 *Biol* 52(7):N127–N135
- 629 Craft DL, Halabi TF, Shih HA, Bortfeld TR (2006) Approximating convex Pareto surfaces in multiobjective  
630 radiotherapy planning. *Med Phys* 33:3399–3407
- 631 D’Souza W, Meyer RR, Shi L (2004) Selection of beam orientations in intensity-modulated radiation therapy  
632 using single-beam indices and integer programming. *Phys Med Biol* 49(15):3465–3481
- 633 Das SK, Marks LB (1997) Selection of coplanar or noncoplanar beams using three-dimensional optimization  
634 based on maximum beam separation and minimized nontarget irradiation. *Int J Radiat Oncol Biol Phys*  
635 38(3):643
- 636 Deasy J, Lee EK, Bortfeld T, Langer M, Zakarian K, Alaly J, Zhang Y, Liu H, Mohan R, Ahuja R (2006)  
637 A collaborative for radiation therapy treatment planning optimization research. *Ann Oper Res* 148(1):  
638 55–63
- 639 Deasy JO, Blanco AI, Clark VH (2003) CERR: a computational environment for radiotherapy research.  
640 *Med Phys* 30:979–985
- 641 Djajaputra D, Wu Q, Wu Y, Mohan R (2003) Algorithm and performance of a clinical IMRT beam-angle  
642 optimization system. *Phys Med Biol* 48(19):3191–3212
- 643 Ehrgott M, Holder A, Reese J (2008) “Beam selection in radiotherapy design”. *Linear Algebra Appl*  
644 428:1272–1312
- 645 Ehrgott M, Johnston R (2003) Optimisation of beam directions in intensity modulated radiation therapy  
646 planning. *OR Spectr* 25(2):251–264
- 647 El-Beltagy MA, Keane AJ (1999) Metamodeling techniques for evolutionary optimization of computa-  
648 tionally expensive problems: promises and limitations. In: *Proceedings of the genetic and evolutionary*  
649 *computation conference*, Orlando, USA, pp 196–203
- 650 Emmerich M, Giotis A, Özdemir M, Bäck T, Giannakoglou K (2002) Metamodel-assisted evolution strate-  
651 gies. *Parallel problem solving from nature PPSN VII*. Springer, Berlin
- 652 Fiege J, McCurdy B, Potrebko P, Champion H, Cull A (2011) PARETO: a novel evolutionary optimization  
653 approach to multiobjective IMRT planning. *Med Phys* 38:5217–5229

- 654 Goitein M, Abrams M, Rowell D, Pollari H, Wiles J (1983) Multi-dimensional treatment planning: II.  
655 Beam's eye-view, back projection, and projection through CT sections. *Int J Radiat Oncol Biol Phys*  
656 9(6):789–797
- 657 Goodband JH, Haas OCL (2008). Artificial neural networks in radiation therapy. *Intell Adapt Syst Med*  
658 213–257
- 659 Gulliford SL, Webb S, Rowbottom CG, Corne DW, Dearnaley DP (2004) Use of artificial neural networks to  
660 predict biological outcomes for patients receiving radical radiotherapy of the prostate. *Radiother Oncol*  
661 71(1):3–12
- 662 Haas OCL, Burnham KJ, Mills JA (1998) Optimization of beam orientation in radiotherapy using planar  
663 geometry. *Phys Med Biol* 43:2179–2193
- 664 Haas OCL, Reeves CR (2005) Genetic algorithms in radiotherapy. *Stud Multidiscip* 3:447–482
- 665 Han J, Kamber M (2006) Data mining: concepts and techniques. Morgan Kaufmann, Burlington
- 666 Holdsworth C, Kim M, Liao J, Phillips MH (2010) A hierarchical evolutionary algorithm for multiobjective  
667 optimization in IMRT. *Med Phys* 37:4986–4997
- 668 Hüsken M, Jin Y, Sendhoff B (2005) Structure optimization of neural networks for evolutionary design  
669 optimization. *Soft Comput A Fusion Found Methodol Appl* 9(1):21–28
- 670 Jin Y, Branke J (2005) Evolutionary optimization in uncertain environments—a survey. *Evol Comput IEEE*  
671 *Trans* 9(3):303–317
- 672 Jin Y, Olhofer M, Sendhoff B (2002) A framework for evolutionary optimization with approximate fitness  
673 functions. *Evol Comput IEEE Trans* 6(5):481–494
- 674 Jin Y, Sendhoff B (2004) Reducing fitness evaluations using clustering techniques and neural network  
675 ensembles. *Genetic and Evolutionary Computation GECCO*. Springer, Seattle
- 676 Kalantzis G, Vasquez-Quino LA, Zalman T, Prax G, Lei Y (2011) Toward IMRT 2D dose modeling using  
677 artificial neural networks: A feasibility study. *Med Phys* 38:5807–5817
- 678 Knezevic A (2008) Overlapping confidence intervals and statistical significance. *StatNews* #73. <http://www.cscu.cornell.edu/news/statnews/stnews73.pdf>. Accessed 14th January 2013
- 679 Knowles J, Gorne D, Bishop M (1998) Evolutionary training of artificial neural networks for radiotherapy  
680 treatment of cancers. *IEEE World Congress on Computational Intelligence*, pp 398–403, Alasca
- 681 Lahanas M, Schreiber E, Milickovic N, Baltas D (2003) Intensity modulated beam radiation therapy dose  
682 optimization with multiobjective evolutionary algorithms. *Evolutionary multi-criterion optimization*,  
683 second international conference, pp 70–70, Springer, Faro, Portugal
- 684 Lee EK, Fox T, Crocker I (2003) Integer programming applied to intensity-modulated radiation therapy  
685 treatment planning. *Ann Oper Res* 119(1):165–181
- 686 Lee EK, Fox T, Crocker I (2006) Simultaneous beam geometry and intensity map optimization in intensity-  
687 modulated radiation therapy. *Int J Radiat Oncol Biol Phys* 64(1):301–320
- 688 Lei J, Li Y (2008). A DNA genetic algorithm for beam angle selection in radiotherapy planning. *Cybernetics*  
689 *and Intelligent Systems*, 2008 IEEE conference on, IEEE, pp 1331–1336
- 690 Li Y, Lei J (2010) A feasible solution to the beam-angle-optimization problem in radiotherapy planning  
691 with a DNA-based genetic algorithm. *Biomed Eng IEEE Trans* 57(3):499–508
- 692 Li Y, Yao D (2006) Accelerating the radiotherapy planning with a hybrid method of genetic algorithm and  
693 ant colony system. *Lect Notes Comput Sci* 4222:340
- 694 Li Y, Yao D, Yao J, Chen W (2005) A particle swarm optimization algorithm for beam angle selection in  
695 intensity-modulated radiotherapy planning. *Phys Med Biol* 50:3491
- 696 Li Y, Yao D, Zheng J, Yao J (2006) A modified genetic algorithm for the beam angle optimization problem  
697 in intensity-modulated radiotherapy planning. *Artif Evol* 97–106
- 698 Li Y, Yao J, Yao D (2004) Automatic beam angle selection in IMRT planning using genetic algorithm. *Phys*  
699 *Med Biol* 49:1915
- 700 Lim GJ (2008). Introduction to radiation therapy planning optimization. *Optim Med Biol* 197–221
- 701 Lim GJ, Cao W (2012) A two-phase method for selecting IMRT treatment beam angles: Branch-and-Prune  
702 and local neighborhood search. *Eur J Oper Res* 217(3):609–618
- 703 Liu HH, Jauregui M, Zhang X, Wang X, Dong L, Mohan R (2006) Beam angle optimization and reduction  
704 for intensity-modulated radiation therapy of non-small-cell lung cancers. *Int J Radiat Oncol Biol Phys*  
705 65(2):561
- 706 Llacer J, Li S, Agazaryan N, Promberger C, Solberg TD (2009) Non-coplanar automatic beam orientation  
707 selection in cranial IMRT: a practical methodology. *Phys Med Biol* 54:1337–1368
- 708 Lu HM, Kooy HM, Leber ZH, Ledoux RJ (1997) Optimized beam planning for linear accelerator-based  
709 stereotactic radiosurgery. *Int J Radiat Oncol Biol, Phys* 39(5):1183–1189
- 710



- 711 Mathieu R, Martin E, Gschwind R, Makovicka L, Contassot-Vivier S, Bahi J (2005) Calculations of dose  
712 distributions using a neural network model. *Phys Med Biol* 50:1019–1028
- 713 Nazareth DP, Brunner S, Jones MD, Malhotra HK, Bakhtiari M (2009) Optimization of beam angles  
714 for intensity modulated radiation therapy treatment planning using genetic algorithm on a distributed  
715 computing platform. *J Med Phys Assoc Med Phys India* 34(3):129
- 716 Pugachev A, Xing L (2001a) Computer-assisted selection of coplanar beam orientations in intensity-  
717 modulated radiation therapy. *Phys Med Biol* 46(9):2467–2476
- 718 Pugachev A, Xing L (2001b) Pseudo beam's eye-view as applied to beam orientation selection in intensity-  
719 modulated radiation therapy. *Int J Radiat Oncol Biol Phys* 51(5):1361–1370
- 720 Pugachev A, Xing L (2002) Incorporating prior knowledge into beam orientaton optimization in IMRT. *Int*  
721 *J Radiat Oncol Biol Phys* 54(5):1565–1574
- 722 Rocha H, Dias J, Ferreira BC, Lopes MC (2012) Selection of intensity modulated radiation therapy treatment  
723 beam directions using radial basis functions within a pattern search methods framework. *J Glob Optim*  
724 (accepted)
- 725 Romeijn HE, Ahuja RK, Dempsey JF, Kumar A, Li JG (2003) A novel linear programming approach to  
726 fluence map optimization for intensity modulated radiation therapy treatment planning. *Phys Med Biol*  
727 48(21):3521–3542
- 728 Rowbottom CG, Webb S, Oldham M (1999) Beam-orientation customization using an artificial neural  
729 network. *Phys Med Biol* 44:2251–2262
- 730 Schreiber E, Lahanas M, Xing L, Baltas D (2004) Multiobjective evolutionary optimization of the  
731 number of beams, their orientations and weights for intensity-modulated radiation therapy. *Phys Med*  
732 *Biol* 49(5):747–770
- 733 Shanker M, Hu MY, Hung MS (1996) Effect of data standardization on neural network training. *Omega*  
734 24(4):385–397
- 735 Stein J, Mohan R, Wang XH, Bortfeld T, Wu Q, Preiser K, Ling CC, Schlegel W (1997) Number and  
736 orientations of beams in intensity-modulated radiation treatments. *Med Phys* 24:149–160
- 737 Vasseur A, Makovicka L, Martin A, Sauget M, Contassot-Vivier S, Bahi J (2008) Dose calculations using  
738 artificial neural networks: a feasibility study for photon beams. *Nucl Instrum Methods Phys Res Sect B*  
739 *Beam Interact Mater Atoms* 266(7):1085–1093
- 740 Wells DM, Niederer J (1998) A medical expert system approach using artificial neural networks for stan-  
741 dardized treatment planning. *Int J Radiat Oncol Biol Phys* 41(1):173–182
- 742 Willoughby TR, Starkschall G, Janjan NA, Rosen II (1996) Evaluation and scoring of radiotherapy treatment  
743 plans using an artificial neural network. *Int J Radiat Oncol Biol Phys* 34(4):923–930
- 744 Witten IH, Frank E (2005) Data mining: practical machine learning tools and techniques. Morgan Kaufmann,  
745 Burlington
- 746 Wu X, Zhu Y, Dai J, Wang Z (2000) Selection and determination of beam weights based on genetic  
747 algorithms for conformal radiotherapy treatment planning. *Phys Med Biol* 45:2547–2558